JOURNAL OF EXPERIMENTAL ZOOLOGY (MOL DEV EVOL) 310B:227–239 (2008)

Visualization of Shell Matrix Proteins in Hemocytes and Tissues of the Eastern Oyster, *Crassostrea virginica*

MARY B. JOHNSTONE[1]*, STEVE ELLIS[2], AND ANDREW S. MOUNT[1]
[1]*Department of Biological Sciences, Clemson University, Clemson, South Carolina*
[2]*Department of Animal and Veterinary Science, Clemson University, Clemson, South Carolina*

ABSTRACT The tissues of the oyster were examined for the presence of shell matrix proteins (SMPs) using a combination of Western, proteomic, and epi-fluorescent microscopy techniques. SMP, including 48 and 55 kDa phosphoproteins, was detected in the epithelial cells of mantle, gill, heart, and adductor muscle and linings of arteries and veins. The 48 kDa SMP circulates continuously within the hemolymph, and is present in the immune system hemocytes. It appears to be secreted from hemocytes on induction of shell repair. We suggest that the 48 and 55 kDa proteins are multifunctional and bridge the process of soft tissue repair and shell formation by mediating cellular activities during immune response as well as interacting with the mineral phase during deposition. *J. Exp. Zool. (Mol. Dev. Evol.) 310B:227–239, 2008.* © 2007 Wiley-Liss, Inc.

How to cite this article: Johnstone MB, Ellis S, Mount AS. 2008. Visualization of shell matrix proteins in hemocytes and tissues of the Eastern oyster, *Crassostrea virginica*. J. Exp. Zool. (Mol. Dev. Evol.) 310B:227–239.

Molluscan shell is a composite of inorganic mineral and organic macromolecules termed the organic matrix. The matrix is presumed to mediate a shell formation because of its close association with the mineral phase (Watabe, '65; Kawaguchi and Watabe, '93) and influence on crystal growth (Wheeler et al., '81, '88; Addadi and Weiner, '85; Belcher et al., '96; Feng et al., 2000; Kono et al., 2000; Thompson et al., 2000). We have previously isolated a class of acidic phosphoproteins from the shell of the Eastern oyster, *Crassostrea virginica,* which have putative biomineralization functions (Wheeler et al., '87; Rusenko et al., '91; Wheeler et al., '91; Mount, '99; Myers et al., 2007). These proteins have estimated molecular weights of 48 and 55 kDa and are chemically and structurally similar, where nearly 85% of their composition is marked by three amino acids, aspartic acid, glycine, and phosphoserine (Rusenko et al., '91; Myers et al., '96; Mount, '99; Johnstone, 2007).

Shell formation occurs at the shell margin in intimate association with the mantle organ. This process can be induced by notching the shell which results in the rapid deposition of new shell with mineralogy identical to a normal shell growth (Mount et al., 2004). Cells of the outer epithelium actively secrete acidic matrix components, among others, near the mantle edge where they are presumed to direct crystal formation through anionic domains (Sudo et al., '97; Suzuki et al., 2004; Gotliv et al., 2005; Myers et al., 2007). Immune system cells have been shown to actively participate in oyster shell formation. Specialized hemocytes containing calcium carbonate crystals were observed to deliver intracellular crystals to the shell mineralization front (Mount et al., 2004). This link between the immune system and shell formation exposes a weakness in the traditional model of the process as exclusively mantle epithelium mediated. Furthermore, shell matrix protein (SMP) has been localized in hemocytes and in association with collagen extruded from these cells

Grant sponsor: South Carolina Sea Grant Consortium.
*Correspondence to: Mary Johnstone, 132 Long Hall, Clemson, SC 29634-0314. E-mail: MBJ@clemson.edu
Received 23 March 2007; Revised 7 August 2007; Accepted 12 October 2007
Published online 28 November 2007 in Wiley InterScience (www.interscience.wiley.com). DOI: 10.1002/jez.b.21206

© 2007 WILEY-LISS, INC.

after induction of shell formation (Patel, 2004). Consequently, we have expanded our research focus to investigate how the shell-derived matrix proteins function outside the mantle, in other cellular and tissue processes, and how these functions may relate to shell formation.

To this end, this study describes a survey of tissues including mantle, gill, heart, adductor muscle, and hemolymph for the presence of SMP. Immuno-histochemical examination and Western analyses of these tissues indicate that oyster SMPs, including the 48 and 55 kDa phosphoproteins, are present in other tissues not typically associated with shell formation. These proteins may act in additional capacities beyond those presumed for the epithelial model of shell formation, particularly that of immune system involvement in the biomineralization process.

METHODS

Shell matrix extraction

The soft oyster tissue was removed from the shells and the shells were scrubbed with a wire brush under tap water. The outer shell layers, including the periostracum and the prismatic layer, were ground away with a hand-held rotary tool. The remaining shell was broken into small pieces, and pieces were composed of foliated mineral were selected and ground into powder by short bursts in an electric coffee grinder. The protein was extracted from the mineral by dissolving 25 g of foliated shell in 750 ml of 17% ethylene diamine tetraacetic acid (EDTA), pH 8. The resulting matrix suspension was centrifuged at 27,000 g relative centrifugal force (RCF) at tip for 30 min to pellet the insoluble material from the water soluble shell matrix. The SMP contained in the supernatant was decanted, concentrated to approximately 50 ml, and then dialyzed against 1,000 ml of 10 mM NaCl using a Pelicon filtration apparatus (Millipore Inc., Billerica, MA) with a molecular weight exclusion limit of 10 kDa. The resultant dialysate was further dialyzed against distilled water three times, lyophilized, and stored at −20°C.

Protein extraction from tissue

Shell repair was induced by notching the shell adjacent to the adductor muscle using a cement saw. Approximately 0.5 ml of hemolymph (blood) was collected from animals before and after induction. Hemocytes were separated from serum by centrifugation at 500 g RCF at tip for 2 min. Serum protein was estimated by bicinchoninic acid (BCA) protein assay (Pierce Inc., Rockford, IL) and stored at −20°C or immediately subjected to Western analysis. Cell pellets were washed three times in 200 µl of calcium-free artificial seawater. After the third wash, 10 µl of reconstituted cells were diluted to 100 µl with distilled water, sonicated, and protein was estimated by BCA. Cells were pelleted then either lyophilized and stored at −20° or subjected immediately to Western analysis. Approximately 1 g pieces of the mantle including the mantle margin, gill, heart, and adductor muscle (including the region of shell attachment) were homogenized in 3 ml of buffer containing 50 mM Tris, pH 7.5, 0.2 mM (EDTA), using an automatic tissue disrupter. This buffer contained variety of protease inhibitors in final concentrations as suggested by the manufacturer (Protease Inhibitor Set, Boehringer Mannheim Inc., Indianapolis, IN). Extracts were centrifuged at 10,000 g RCF at tip for 10 min and the supernatant was dialyzed against three changes of distilled water, overnight at 4°C. The protein quantity was estimated with BCA, and aliquots were stored at −20°C.

Antibody preparation

A polyclonal antibody to SMP (anti-SMP) was prepared commercially in rabbit hosts (Zymed Inc., Carlsbad, CA). Serum was stored in 1 ml aliquots at −20°C. A portion of anti-SMP serum was affinity purified against the 48 kDa phosphoprotein using the MicroLink protein coupling kit (Pierce). The 48 kDa protein was purified from the shell matrix extract on 4–20% preparative sodium dodecyl sulphate-polyacrylamide gel electrophoresis (SDS-PAGE) gels (Invitrogen Inc., Carlsbad, CA) and eluted using a micro-eluter (Bio-Rad Inc., Hercules, CA). Eluted 48 kDa protein was coupled to the column with an estimated coupling efficiency of 87%. Eluent was monitored by enzyme-linked immunosorbent assay and those with the highest titer to 48 kDa were pooled, stabilized with bovine serum albumin (BSA) to 3%, and preserved with sodium azide to 0.02%. The affinity purified anti-48-kDa antibody was stored at 4°C.

Histochemical analysis

Before histochemical analysis, oysters were perfused and fixed intact with 4% paraformaldehyde in phosphate buffered saline (PBS), pH 7.4. PBS was adjusted using 1 M NaCl, to match osmolality of the holding tank at the time of tissue

harvest. Tissue was embedded in Immunobed™ (Poly Sciences Inc., Warrington, PA) and sectioned at 1–1.5 μm. Sections were stained using Azure II (Fritsch, '89).

Immuno-histochemical imaging was carried out using the affinity purified anti-48 kDa isolated from the anti-SMP serum. Immuno-staining was carried out using antibodies diluted in PBS, pH 7.4 containing 1% BSA and 0.1% Triton ×100. This buffer was also used as the wash buffer. The anti-48-kDa antibody was diluted to 1:700. Before immuno-staining, slides were rehydrated through a graded series of alcohol solutions in distilled water, starting with 100% ethyl alcohol and ending with PBS for 2 min each. Slides were blocked in the PBS buffer containing 5% BSA, 10% normal goat serum (Sigma-Aldrich Inc., St. Louis, MO) and 0.1% Triton ×100, for 6 hr at room temperature. After a brief rinse in PBS, slides were incubated in primary antibody solutions overnight at 4°C. Washes after the primary and secondary incubations were carried out three times for 10 min each. Immuno-reactivity was detected using Alexafluor 488 goat anti-rabbit fluorescent antibody (Molecular Probes Inc., Eugene, OR) at a concentration of 6 μg/ml. Control experiments were carried out using pre-immune serum (1:1,000) to assess background staining. Additional sections were stained with anti-SMP at 1:1,000. All incubations were carried out in a covered humid chamber with gentle agitation. Sections were mounted in a 1:1 solution of glycerol and PBS, pH 7.4, and then examined with a Zeiss Axiovert 135 inverted fluorescent microscope (Carl Zeiss MicroImaging., Thornwood, NY) equipped with a SPOT-RT Cooled Color CCD camera (Diagnostic Instruments Inc., Sterling Heights, MI).

Western analysis

Cell pellets were reconstituted in the SDS-PAGE sample buffer, sonicated for 1 min, and heated for 2 min at 90°C. Tissue homogenates, serum, and cell lysates were resolved on 4–20% poly-acrylamide gradient SDS-PAGE gels (Invitrogen) and transferred onto nitrocellulose. Transfer was conducted for 1 hr at 100 V in buffer containing 25 mM Tris, 192 mM glycine, 20% v/v methanol, and pH 8.3 using a mini-transfer unit (Invitrogen). After the transfer, membranes were rinsed once with Tris buffered saline (TBS), pH 7.5, then placed into 50 ml 3% BSA and 1% goat serum in TBS (blocking buffer) and incubated overnight at 4°C. After blocking, membranes were incubated in 25 ml of the anti-SMP antibody diluted 1:1,000 in 3% BSA in TBS (western buffer) for 2 hr. Membranes were washed three times in 100 ml of 1% BSA and 0.05% Tween-20 in TBS (wash buffer) for 5 min each. The membrane was incubated in 25 ml of alkaline–phosphatase conjugated goat anti-rabbit IgG (Sigma) diluted to 1:30,000 in western buffer for 1.5 hr, and subsequently washed three times for 5 min each in wash buffer. Except for the blocking step, all incubations and washes were carried out with continuous gentle shaking at room temperature. A final rinse was carried out in TBS and color was developed with BCIP/NBT (Sigma). Development was stopped by repeated washing in distilled water.

Peptide sequencing of 48 kDa phosphoprotein

Extracts of shell, hemocytes, and serum were resolved on 4–12% Bis-Tris gels (Invitrogen), and the 48 kDa bands were excised and subjected to mass spectral analysis. Approximately 1 ml of hemolymph was drawn from three specimens and was centrifuged at 500 g RCF at tip for 2 min to separate the cells from the serum. Cell pellets were resuspended in 10 μl of distilled water containing 2% SDS to lyse the cells. Extracts were pooled, split into two equal volumes and applied in duplicate to the gel in sample buffer. Twenty microlitres of serum and approximately 50 μg of dry weight SMP were applied in duplicate to the gel. All samples were sonicated and heated before electrophoresis. One half of the gel was stained with Stains-all to identify the 48 kDa band in shell matrix. The remaining half of the gel was stained with zinc stain (Bio-Rad). By placing the gels side by side, the Stains-all positive 48 kDa band was used as a reference, along with molecular weight markers, to clearly identify the 48 kDa proteins on the zinc stained gel. The 48 kDa bands identified in hemocytes, serum, and shell matrix were excised from this gel, destained and submitted to the Proteomics Center at the Medical University of South Carolina. There, proteins were digested with Asp-N endoproteinase and peptides resulting from this treatment were analyzed by mass spectrometry. Sequences were searched against GenBank (National Center for Biotechnology Information, Bethesda, MD; www.ncbi.nlm.nih.gov/Genbank/Genbanksearch.html) and the marine genomics data bank (www.marinegenomics.org).

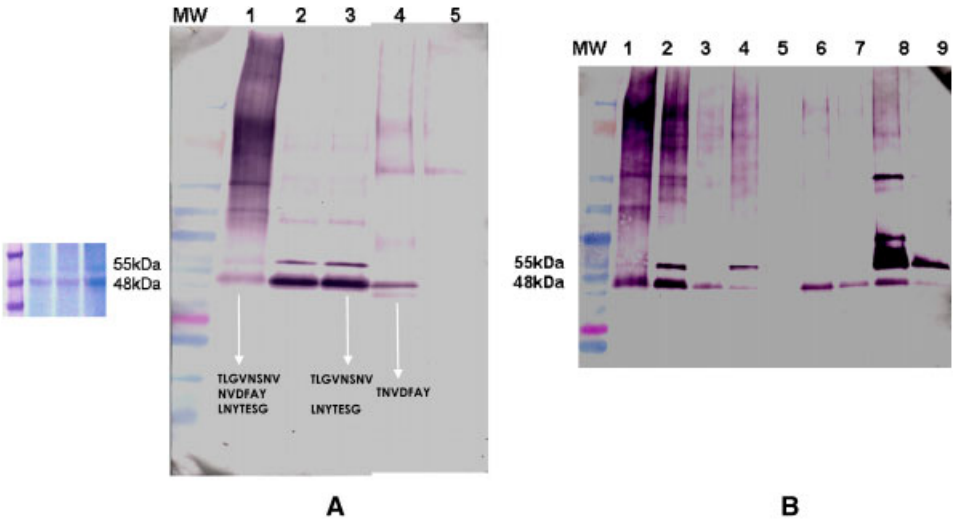

Fig. 1. Western blot analyses of shell matrix and tissue extracts. (**A**) The 48 and 55 kDa phosphoproteins, present in shell matrix (lane 1 and inset on left), were identified in the serum and hemocytes of hemolymph collected before and after induction of shell repair. Proteins were detected using an antibody made to whole water soluble shell matrix (anti-SMP). Protein was estimated for cell lysates and serum using BCA protein assay. Approximately 10 μg of protein was loaded per lane. Molecular weight (MW) was estimated from SeeBlue Plus 2 protein standards (Invitrogen). The middle section of the blot was removed. Inset (on left) shows the 48 and 55 kDa phosphoproteins resolved on a 4–20% gradient Tris-glycine ready gel (Invitrogen) following stains-all staining. Lane assignments are; 1, shell matrix, 10 μg dry weight, with peptide sequences determined from the 48 kDa protein shown below; 2, serum (control); 3, serum (induced) and two peptides determined for the 48 kDa band; 4, hemocyte lysate (control) with one peptide determined for the 48 kDa band; 5, hemocyte lysate (induced). (**B**) Western analyses of selected tissue extracts demonstrating the presence of shell matrix protein; the 48 and 55 kDa proteins are indicated. Tissue samples were loaded in paired lanes with 10 and 1 μg, respectively. Protein was detected using the anti-SMP antibody. MW was estimated from SeeBlue Plus 2 protein standards (Invitrogen). Lane assignments are; 1, shell matrix, 10 μg dry weight; 2 and 3, mantle; 4 and 5, heart; 6 and 7, gill; 8 and 9, adductor muscle.

RESULTS

Western analyses

Shell matrix

The anti-SMP antibody recognizes several discrete protein bands in shell matrix extract (Fig. 1A; lane 1) including the 48 and 55 kDa phosphoproteins, which are identified by Stains-all stain following SDS-PAGE (Fig. 1 inset). These proteins have highly related structures and are members of an acidic class of proteins identified previously in oyster shell matrix. (Rusenko et al., '91; Myers et al., '96; Myers et al., 2007; Johnstone, 2007).

Hemolymph

Hemolymph is the circulatory fluid of the oyster and consists of immune cells and serum. The serum contains proteins, lipids, carbohydrates, and humoral factors such as agglutinins and lysins (Cheng, 1996). Western blot analysis of serum, collected before (control) and after induction of shell repair, indicates that the 48 and 55 kDa proteins are present in both collections (Fig. 1A; lanes 2 and 3) and demonstrates that both proteins circulate continuously in hemolymph. In contrast, Western analysis of hemocytes shows that the 48 kDa protein is present only in control hemolymph (Fig. 1A; lane 4), and its presence is greatly reduced after the induction of shell repair (Fig. 1A; lane 5). Notably, the 55 kDa protein is not detected in control or induced hemocytes and apparently is produced elsewhere.

Mass spectral sequence analyses

To verify that the anti-SMP antibody identified the 48 kDa phosphoprotein within the tissues tested, the 48 kDa protein bands were isolated from hemocytes and serum, partially sequenced using mass spectral analysis, and compared with sequence determined from the 48 kDa protein derived from shell matrix (control). Matching sequences are noted on Figure 1A. The 48 kDa protein derived from hemocytes and serum share sequence identity with the 48 kDa matrix protein identified in shell.

Tissue homogenates

Western blot analysis of selected tissue homogenates using the anti-SMP antibody detected the presence of SMP, including the 48 and 55 kDa proteins, in a broad range of tissues (Fig. 1B). The mantle (Fig. 1B; lanes 2 and 3), heart (Fig. 1B; lanes 4 and 5), and adductor muscle (Fig. 1B; lanes 8 and 9) stained positive for both the 48 kDa and 55 kDa proteins, whereas the gill (Fig. 1B; lanes 6 and 7) is positive for only the 48 kDa protein. On the basis of staining intensity, the 55 kDa protein is most prominent in the adductor muscle tissue and appears to be roughly two to three times greater in quantity relative to the 48 kDa protein in adductor and heart tissues. The mantle appears to have both proteins in essentially equal amounts.

Besides the 48 and 55 kDa proteins, the anti-SMP antibody reacts with additional bands in the mantle and adductor muscle extracts at higher protein concentrations (lanes 2 and 8). Because similar bands are also visible in shell matrix (lane 1), this reactivity indicates that these tissues have common proteins. This is especially evident in mantle extract and is consistant with the fact that proteins produced in the mantle are incorporated into the shell (Sudo et al., '97). The additional reactive bands in the adductor muscle tissue may be explained by the fact that this organ system is comprised of three tissues including, hemolymph (this organ acts as a hemolymph pressurizer), muscle, and the epithelium that attaches to the shell which produces a unique shell layer, the myostracum (Galstoff, '64).

To increase specificity for the acidic class of SMP, including the 48 and 55 kDa proteins, immuno-histochemical staining was carried out using an affinity purified anti-48 kDa. This antibody resulted in significantly lower background immuno-staining of histological sections compared with the anti-SMP antibody.

Immuno-histochemistry

Mantle

The mantle organ forms the integument of the oyster and is involved in shell formation (Galstoff, '64). The most active zone of shell deposition is along the periphery of the mantle, where it divides into three distinct lobes near the shell edge. There is an outer or extrapallial lobe (OL), which is closest to the shell, a middle tentacle bearing lobe, and an inner or pallial lobe. The region between the OL and middle lobe is termed the periostracal groove (PG). This region terminates into a glandular epithelium, which produces a membranous sheet called the periostracum.

The anti-48 kDa reactivity is confined to the OL epithelium, including the OL portion of the PG (Fig. 2A and B), and the entire shell facing surface of the outer mantle epithelium. The location of SMP in this region of the mantle is consistent with its eventual incorporation into the shell. A control section of the OL was stained with pre-immune serum and shows no specific reactivity above background staining (Fig. 2C).

Heart

The three chambered heart consists of two atria and a common ventricle and is suspended within a thin-walled chamber termed the pericardial coelom (Galstoff, '64). A cross section through the ventricle following Azure Blue II staining reveals the outer protective layer, the epicardium, which consists of simple cuboidal cells and a basement membrane (Fig. 3A). Figure 3B shows the interior of the ventricle, the myocardium, which is composed of a fibrous network of cardiac muscle cells and hemocytes. Following immuno-staining, the epicardium is highly reactive to the anti-48 kDa antibody (Fig. 3C and D) compared with the control section (Fig. 3E) indicating the presence of SMP. The myocardium is not reactive above background staining (Fig. 3F).

Gill

The gills primarily function in respiration and feeding. Each gill consists of two folds of tissue called demibranchs. Each demibranch has a V shape, with each arm of the V forming a lamella (Galstoff, '64). Viewed at low magnification (Fig. 4A), an Azure II-stained longitudinal section reveals the anterior region of a single gill lamella termed the plicae (Fig. 4B). Posterior to the plicae are regions of tissue and water channels (Fig. 4C), which run toward the interior of the lamella structure. Hemolymph circulates in sinuses within the tissues of both regions. Water chambers are evident as the clear spaces posterior to the plica. Hemolymph stains a distinct, neon/light blue color and collects in sinuses located in the interior region of each plica, and in a vessel which runs horizontally (Fig. 4B). Hemolymph also circulates within tissue sinuses which run toward the interior of the gill lamellae (Fig. 4C). Cilia and

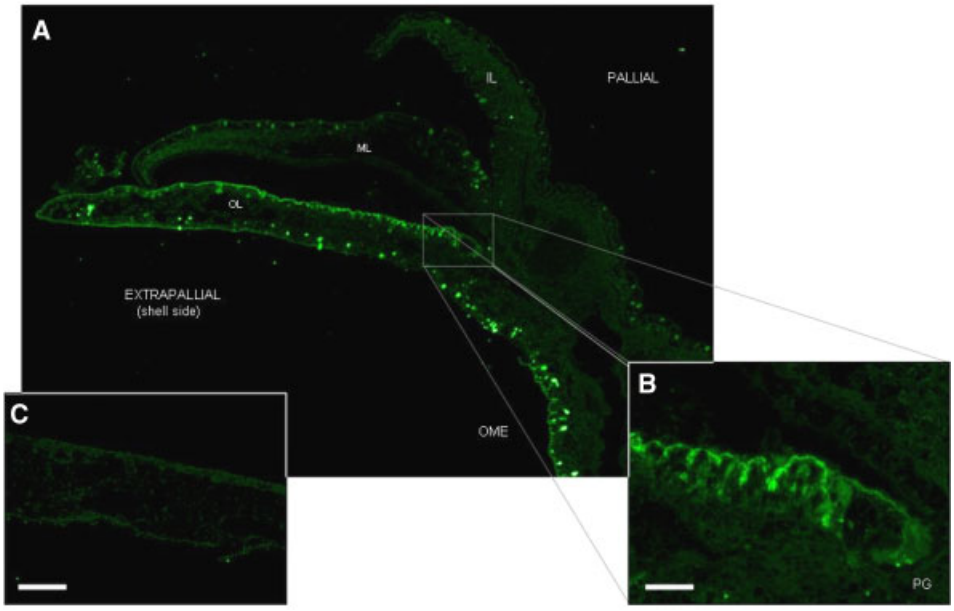

Fig. 2. Transverse section of mantle demonstrating anti-48-kDa antibody immuno-reactivity. (**A**) Mantle from flat valve side of oyster. The outer or extrapallial lobe (OL) is closest to the shell, followed by a middle tentacle bearing lobe (ML), and an inner or pallial lobe (IL). The region between the OL and ML is termed the periostracal groove (PG) and the entire shell facing surface of the extrapallial side is the outer mantle epithelium (OME). Shell matrix protein is secreted from the OL, starting from the PG. Immuno-reactive hemocytes are visible within the OME and along the pallial region of the mantle. (**B**) Enlargement of PG region boxed in (**A**). Staining is restricted the cells of the OL epithelium and a line of intense staining is observed on the apical surface, bar = 40. (**C**) Control section of OL stained with pre-immune serum shows no specific staining, bar = 100 μm.

mucous are present on the anterior surface of each plica, which also stains neon blue (Fig. 4B).

After immuno-staining with the anti-48 kDa antibody (Fig. 5), the entire gill structure stains broadly, but an enhanced reactivity is observed in the inner epithelial linings and in regions where hemolymph collects. The highest immuno-reactivity is observed in the interior region of the plicae near the base (Fig. 5A) and continues, a little less reactive, along the epithelial linings (Fig. 5B). Hemocytes cells show intense reactivity, which are magnified in Figure 5D. Tissue in the interior region of the lamella (Fig. 5C) is reactive and includes hemolymph, epithelial cells, and connective tissue. SMP associates with hemolymph, hemocytes, and with the epithelial linings of the gills. Control sections show low background staining (Fig. 5E and F).

Adductor muscle

The single adductor muscle opens and closes the shell. This structure is comprised of two distinct regions—a translucent region consisting of fast twitch cells and an opaque region of slow twitch fibers (Galstoff, '64). Azure II staining of the translucent region in cross section reveals muscle fibers running perpendicular to the epithelial region of shell attachment (Fig. 6A). Muscle fibers in this region are uninucleate with an elongated appearance. A thin layer of connective tissue called endomysium surrounds each muscle fiber. A thicker layer, the perimysium, surrounds fiber bundles. The anti-48 kDa antibody (Fig. 6B and C) indicates that SMP localizes in the endomysium (Fig. 6B; open arrow) and perimysium of translucent muscle. (Fig. 6C; closed arrow). Notably, immuno-reactivity to the epithelium of the adductor muscle is highest on the shell side (Fig. 6C; see arrow), indicating that SMP localizes in the region of shell attachment. A control section from the muscle exhibits low background staining (Fig. 6D).

Vessels

The walls of arteries and veins are composed of connective tissue fibers and cells. Vessel linings identified in the mantle and adductor muscle are highly reactive to the anti-48 kDa antibody (Fig. 7A and C). A reactive material thought to be hemolymph was identified in a mantle sinus (Fig. 7B). These sections show that SMP concentrates in the vessel linings and in the hemolymph filled sinuses. These structures were not visible in control sections.

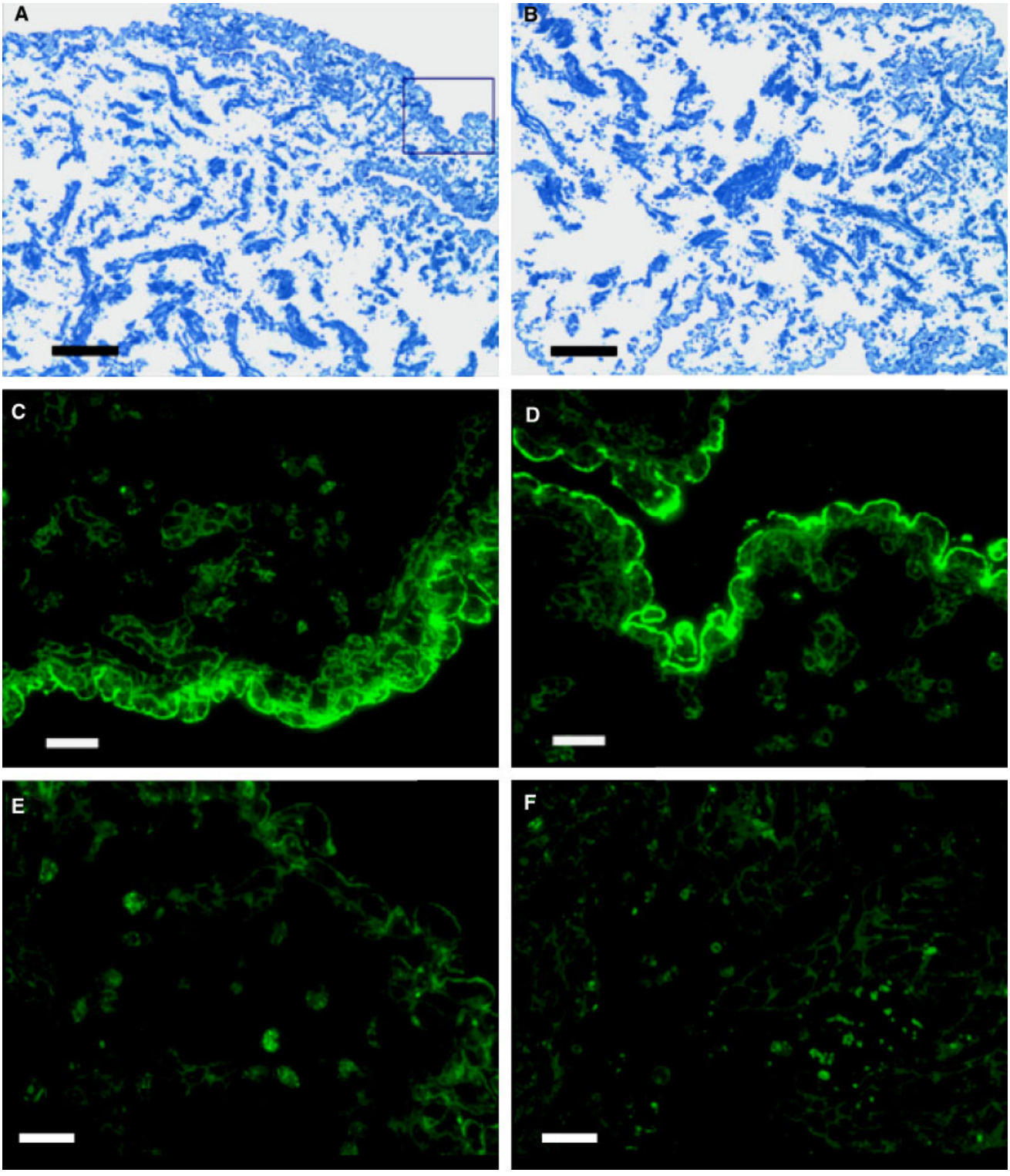

Fig. 3. Cross section through the ventricle of the heart. (**A**) Heart margin (epicardium) and associated epithelium (upper right) and its interior region, the myocardium, bar = 300 μm. (**B**) Myocardium of the heart illustrating the porosity of the tissue, bar = 200 μm. (**C**) and (**D**) Immuno-staining with anti-48-kDa antibody of the boxed region in (**A**), bar = 100 μm. Antibody reactivity is confined to the epithelium of the epicardium. (**E** and **F**) Control sections stained with pre-immune serum of the epicardium and myocardium, respectively, bar = 100 μm. Compared with (**C**) and (**D**), controls show that the myocardium and epicardium are not reactive.

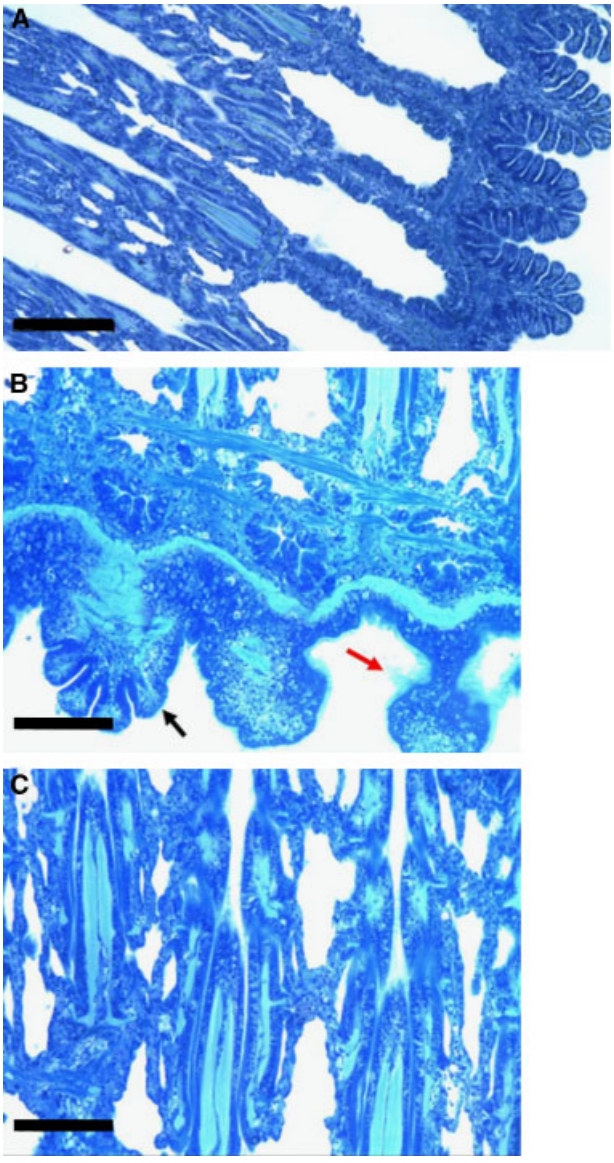

Fig. 4. Transverse (or frontal) sections of the gill lamellae stained with Azure II. (**A**) Low magnification showing anterior gill region, bar = 320 μm (**B**) Anterior region showing three gill plicae, the black arrow denotes one gill plica, bar = 200 μm. Hemolymph stains light blue and collects at the base of each plica as well as in a vessel that runs horizontally. Mucous and cilia present on the surface (red arrow) also stain light blue. (**C**) Interior region of gill showing hemolymph filled vessels which run vertically toward the posterior of the gill, bar = 200 μm.

DISCUSSION

In this study, we examined the major tissues of the oyster for the presence of SMP. We found that SMP is present in the outer lobe of the mantle epithelium as well as the epithelium of organ systems including the gill, heart, adductor muscle, and vessel linings. Western and mass spectral analyses demonstrated that the 48 and 55 kDa phosphoproteins, characterized previously from oyster shell matrix (Rusenko et al., '91; Myers et al., '96; Myers et al., 2007; Johnstone, 2007), are among the proteins detected in these tissues. Both proteins were shown to be consistent components of hemolymph serum, but only the 48 kDa protein seems to be expressed by hemocytes, which are the oyster's immune system cells and facilitate tissue repair (Humphries and Yoshino, 2003).

After shell induction, the 48 kDa protein is not visible in hemocytes. We interpret this observation to indicate that this protein is regulated by hemocyte cells in response to shell formation and is compelling evidence for direct involvement of the immune system in biomineralization. The protein seems to be constitutively expressed by hemocytes and deployed after induction of shell repair. This would explain its presence in both serum collections. Patel (2004) has shown that after induction of shell repair, hemocytes secrete collagen fibers coated with SMP. The simultaneous release of this SMP–collagen complex from induced cells may account for the decline of the 48 kDa protein from hemocytes. Also, the peptide sequence (TNVDFAY), identified in the 48 kDa protein in hemocytes and shell matrix, shares homology with an immune response protein identified from an expressed sequence tag (EST) from *Crassostrea gigas* hemocytes (Gueguen et al., 2003). These data, considered with the finding that hemocytes supply seed crystals to the mineralization front (Mount et al., 2004), are further evidence that the processes of shell and tissue repair are related.

Epithelial tissues of the outer mantle epithelium, the PG and the adductor muscle epithelia secrete SMP, including the 48 and 55 kDa proteins, which are incorporated into the shell organic matrix. The fact that these proteins are restricted to the outer mantle lobe is consistent with a role in shell formation (Sudo et al., '97; Takeuchi and Endo, 2006). However, the association of this protein with the hemocyte infused connective tissues of the endomysium and perimysium of adductor muscle fibers and with heart, gills, and blood vessel linings suggests it has fundamental roles beyond shell formation. This finding is consistent with the recent work of Tirapé et al. (2007), who suggested that hematopoietic cells are derived from vessels and/or artery endothelial cells. Furthermore, the observed differences in the presence and abundance of this protein within the tissues as surveyed by Western

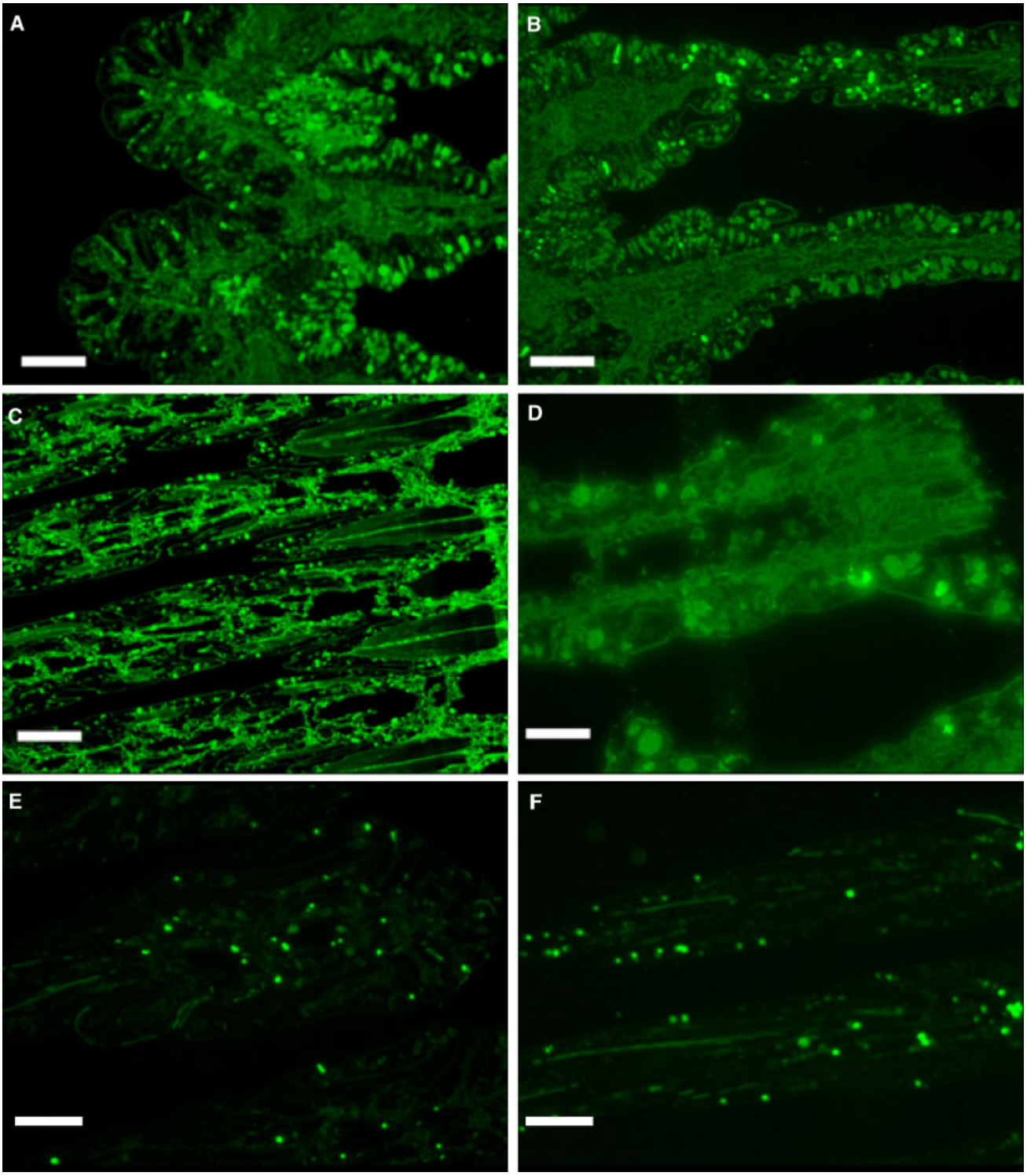

Fig. 5. Immuno-staining of the gill with anti-48-kDa antibody. (**A**) Gill plicae, bar = 100 μm, high reactivity is observed at the base of the plica where hemolymph collects. (**B**) Region just behind the plica, antibody reactivity localizes in the epithelium, bar = 100 μm. (**C**) Interior of gill showing antibody reactivity with hemolymph, epithelial cells, and connective tissue, bar = 100 μm. (**D**) Same region as in (**B**) showing antibody reactive hemocytes, bar = 40 μm. (**E** and **F**) Control sections of similar regions in (**A**) and (**C**) were stained with pre-immune serum and result in low background reactivity.

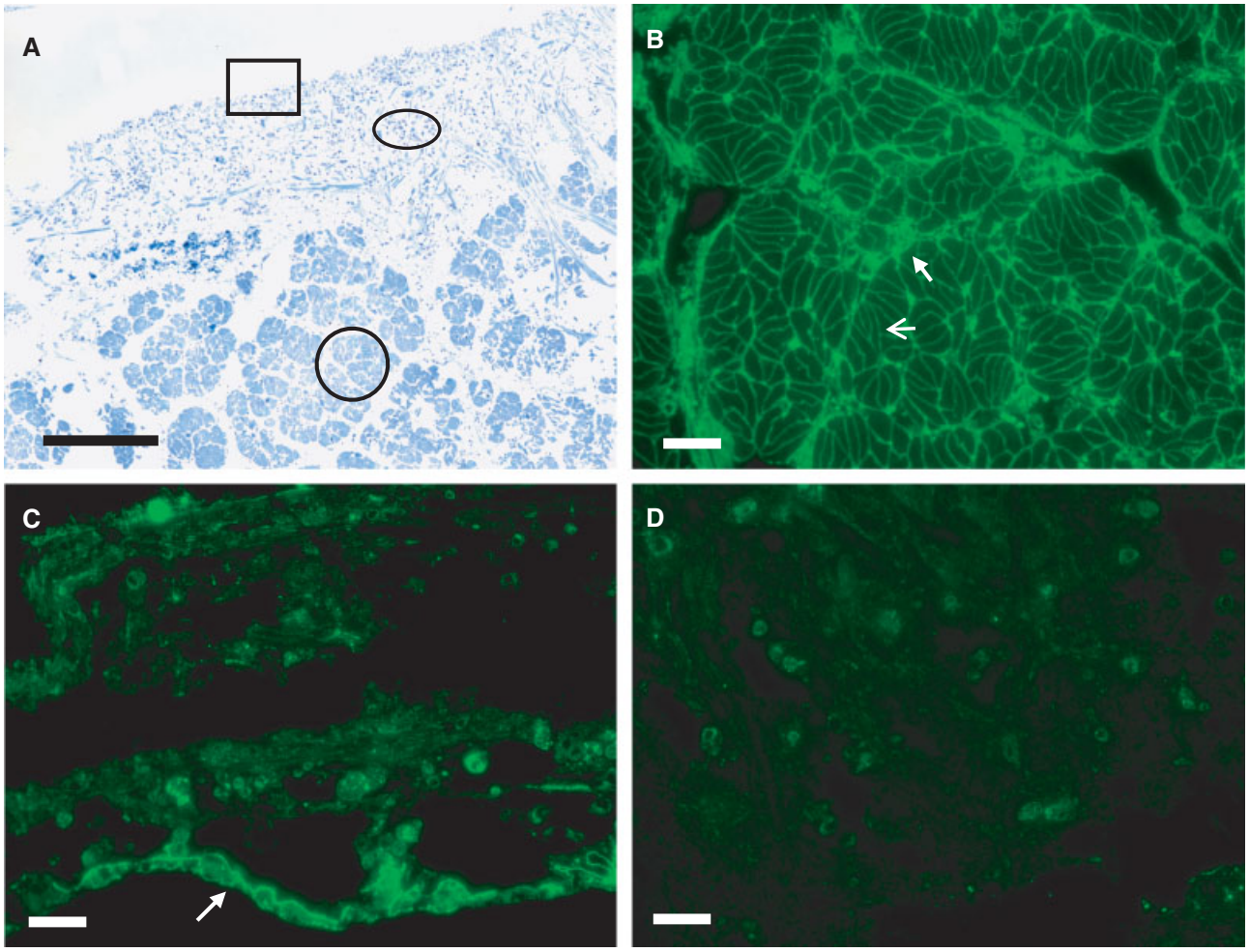

Fig. 6. Immuno-reactivity of adductor muscle and its associated epithelium with the anti-48-kDa antibody. (**A**) Azure II stained transverse section of adductor muscle showing the muscle fiber bundles and epithelium to which the shell is attached, bar = 320 μm. (**B**) Immuno-reactivity of adductor muscle region, circled in (**A**). The open arrow points to shell matrix protein (SMP) associated with endomysium. The closed arrow shows localization of the SMP to perimysium, bar = 40 μm. (**C**) Adductor muscle epithelium region, boxed in (**A**), stained with anti-48 kDa antibody. The arrow indicates SMP is present in the adductor epithelium, which is the site of muscle to shell attachment (arrow), bar = 40 μm. (**D**) Control section of adductor muscle stained with pre-immune serum indicates low background reactivity. The oval in (**A**) indicates the region, bar = 40 μm.

analysis suggest its roles are specialized and regulated.

The presence of SMP in a variety of organ systems including hemocytes suggests some of them, including the 48 and 55 kDa, are multi-functional. Evidence is mounting that molluscan shell isolates carry out varied functions with the discovery of domains like that in nacrein, a matrix protein that has a functional carbonic anhydrase domain (Kono et al., 2000; Miyamoto et al., 2005) and perlucin, a matrix protein that has a C-type lectin domain and binds calcium (Mann et al., 2000) as well as enhances initiation of crystal growth (Weiss et al., 2000). A mucin with anti-mineralizing properties has been identified from the nacre of *Pinna noblis* (Marin et al., 2000), and may have immune function (Agrawal et al., '98). Shell proteins derived from the nacre of two species, *Pinctada maxima* and *Pinctada fucata*, have been shown to have regulatory activities on mineralogenic cells lines (Almeida et al., 2000, 2001; Sud et al., 2001; Mouries et al., 2002; Zhang et al., 2006).

This study shows the presence of SMP outside the mantle organ, which has not been previously reported for shell protein isolates (Zhang and Zhang, 2006). However, recent findings show that gene isolates, identified in the mantle and presumed to be involved in shell formation, have been detected in other tissues including the adductor

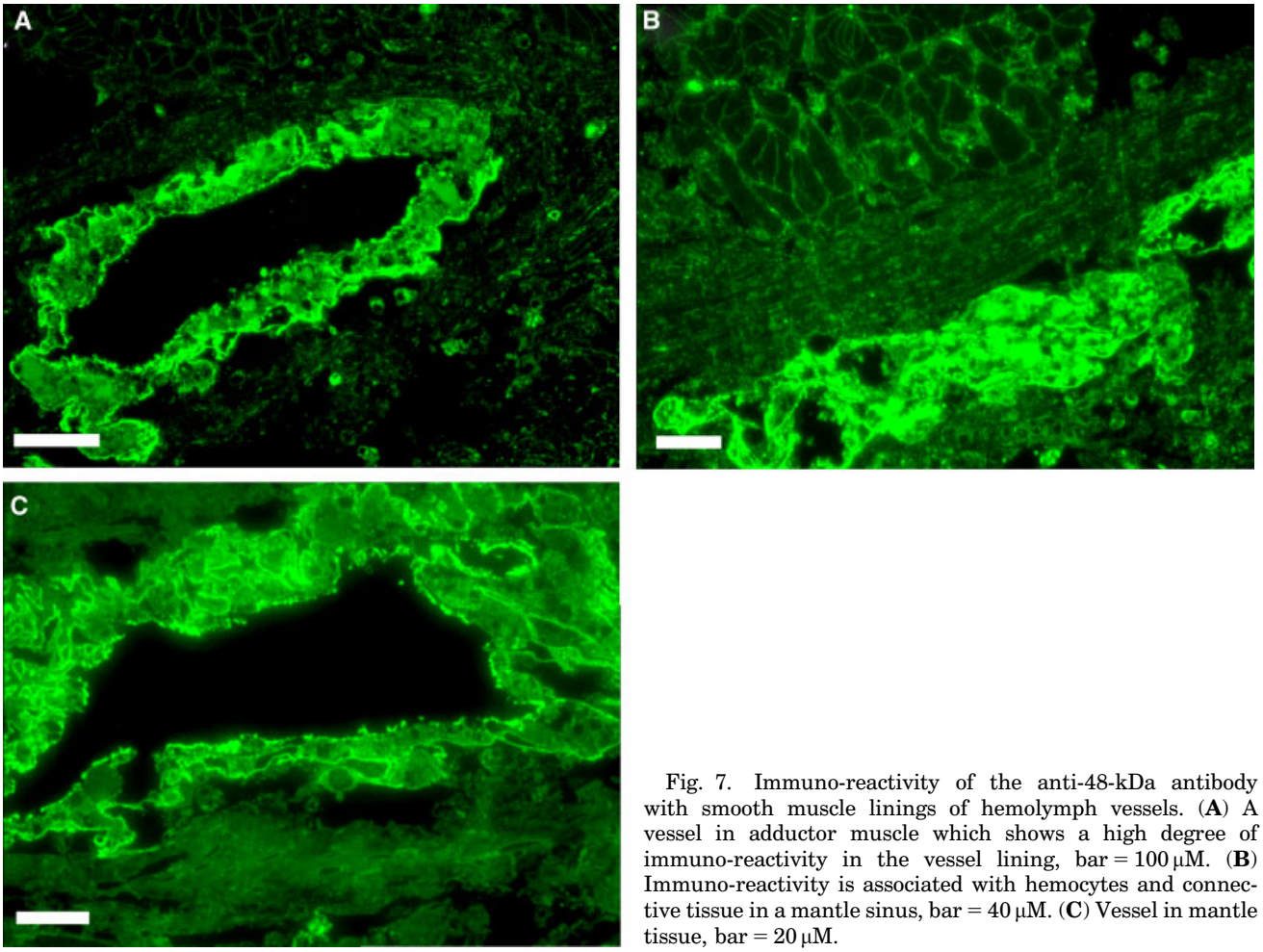

Fig. 7. Immuno-reactivity of the anti-48-kDa antibody with smooth muscle linings of hemolymph vessels. (**A**) A vessel in adductor muscle which shows a high degree of immuno-reactivity in the vessel lining, bar = 100 μM. (**B**) Immuno-reactivity is associated with hemocytes and connective tissue in a mantle sinus, bar = 40 μM. (**C**) Vessel in mantle tissue, bar = 20 μM.

muscle (Yano et al., 2006; Liu et al., 2007), gills, and hemocytes (Huang et al., 2007).

Although a broad distribution of mineral-derived matrix protein is a new observation in studies of shell formation, it is well documented for osteopontin (OPN), a matrix protein involved in the formation of vertebrate teeth and bone. OPN occurs in a variety of tissues and has multiple functions beyond mineral deposition. Like the 48 and 55 kDa shell proteins, OPN is a major constituent of the mineralized matrix of bone. It has been chemically likened to oyster shell SM protein (Zhang and Zhang, 2006) and behaves similarly in assays testing crystal formation and growth (Wheeler et al., '81; Borbas et al., '91; Hunter and Goldberg, '93, '94; Boskey et al., '93; Mount, '99;Wada et al., '99; Gericke et al., 2005). OPN organizes osteogenic cells during bone formation by simultaneously binding to collagen and cells through RGD domains, and mineral through anionic domains (Sodek et al., 2000).

OPN's broad distribution is comparable to SMP in oyster tissues. It is widely expressed by epithelial cells at the luminal surfaces of a variety of organs and glands as well as gastrointestinal and reproductive tracts in humans (Brown et al., '92). It acts as an anti-mineralizing agent, preventing ectopic calcification of soft tissues (Giachelli, 2001; Steitz et al., 2002). OPN is secreted by activated macrophages, T lymphocytes and leukocytes, and circulates in serum and is elevated in most tissues during wound healing (Giachelli and Steitz, 2000; Gravallese, 2003). As a cytokine, it binds to an array of integrins thereby stimulating cell adhesion, migration, signaling, and survival mechanisms for a variety of mesenchymal, epithelial, and inflammatory cells (Giachelli et al., '98; Giachelli and Steitz, 2000; O'Regan and Berman, 2000; Gravallese, 2003; Zhu et al., 2004).

The occurrence of SMP in a variety of somatic tissues, including blood serum and hemocytes, fits well with an OPN model of multi-functionality.

We propose that SMP, including the 48 and 55 kDa proteins, bridge the process of soft tissue repair and shell formation by mediating cellular activities during immune response as well as interacting with the mineral phase during deposition. Given the wealth of studies documenting multifunctional, mineral-derived proteins in vertebrate and invertebrate species and their demonstrated immune functions, our findings warrant serious consideration. Immune system driven cellular biomineralization implies the production of calcified hard parts is conserved. Future studies in molluscan shell formation are likely to uncover more links to immunity thus revealing a better understanding of the evolution of biomineralization in both phyla.

ACKNOWLEDGMENTS

We thank Dr. Kevin L. Schey and Jennifer R. Bethard, at the Proteomics Center at Medical University of South Carolina, for generously providing mass spectral data. We also thank Dr. A.P. Wheeler for his comments on the manuscript.

LITERATURE CITED

Addadi L, Weiner S. 1985. Interactions between acidic proteins and crystals: stereochemical requirements in biomineralization. Proc Natl Acad Sci USA 82:4110–4114.

Agrawal B, Gendler SJ, Longenecker BM. 1998. The biological role of mucins in cellular interactions and immune regulation: prospects for cancer immunotherapy. Mol Med Today 9:397–403.

Almeida MJ, Milet C, Peduzzi J, Pereira L, Haigle J, Barthelemy M, Lopez E. 2000. Effect of water-soluble matrix fraction extracted from the nacre of *Pinctada maxima* on the alkaline phosphatase activity of cultured fibroblasts. J Exp Zool 288:327–334.

Almedia MJ, Pereira L, Milet C, Haigle J, Barbosa M, Lopez E. 2001. Comparative effects of nacre water-soluble matrix and dexamethasone on the alkaline phosphatase activity of MRC-5 fibroblasts. J Biomed Mater Res 57:306–312.

Belcher AM, Wu XH, Christensen RJ, Hansma PK, Stucky GD, Morse DE. 1996. Control of crystal phase switching and orientation by soluble mollusc-shell proteins. Nature 381: 56–58.

Borbas JE, Wheeler AP, Sikes CS. 1991. Molluscan shell matrix phosphoproteins: correlation of degree of phosphorylation to shell mineral microstructure and to in vitro regulation of mineralization. J Exp Zool 258:1–13.

Boskey AL, Maresca M, Ullrich W, Doty SB, Butler WT, Prince CW. 1993. Osteopontin-hydroxyapatite interactions in vitro: inhibition of hydroxyapatite formation and growth in a gelatin-gel. Bone Miner 22:147–159.

Brown LF, Berse B, Van de Water L, Papadopoulos-Sergiou A, Perruzzi CA, Manseau EJ, Dvorak HF, Senger DR. 1992. Expression and distribution of osteopontin in human tissues: widespread association with luminal epithelial surfaces. Mol Biol Cell 10:1169–1180.

Cheng TC. 1996. Hemocytes: forms and functions. In: Kennedy VS, Newell RE, Eble AF, editors. The Eastern oyster, *Crassostrea virginica*. College Park: Maryland Sea Grant College, University of Maryland System. p 299–326.

Feng QL, Pu G, Pei Y, Cui FZ, Li HD, Kim TN. 2000. Polymorph and morphology of calcium carbonate crystals induced by proteins extracted from mollusk shell. J Crystal Growth 216:459–465.

Fritsch H. 1989. Staining of different tissues in thick epoxy resin-impregnated sections of human fetuses. Stain Technol 64:75–79.

Galstoff PS. 1964. The american oyster. Fishery Bulletin 64, US Department of Interior.

Gericke A, Qin C, Spevak L, Fujimoto Y, Butler WT, Sorensen ES, Boskey AL. 2005. Importance of phosphorylation for osteopontin regulation of biomineralization. Calcif Tissue Int 77:45–54. Epub.

Giachelli CM. 2001. Ectopic calcification: new concepts in cellular regulation. Z Kardiol 90(Suppl 3):31–37.

Giachelli CM, Steitz S. 2000. Osteopontin: a versatile regulator of inflammation and biomineralization. Matrix Biol 7:615–622.

Giachelli CM, Lombardi D, Johnson RJ, Murry CE, Almeida M. 1998. Evidence for a role of osteopontin in macrophage infiltration in response to pathological stimuli in vivo. Am J Pathol 152:353–358.

Gotliv BA, Kessler N, Sumerel JL, Morse DE, Tuross N, Addadi L, Weiner S. 2005. Asprich: a novel aspartic acid rich protein family from the prismatic shell matrix of the bivalve Atrina rigida. Chembiochem 6:304–314.

Gravallese EM. 2003. Osteopontin: a bridge between bone and the immune system. J Clin Invest 112:147–148.

Gueguen Y, Cadoret JP, Flament D, Barreau-Roumiguière C, Garnier J, Girardot AL, Hoareau A, Bachère E, Escoubas JM. 2003. Immune gene discovery by expressed sequence tags generated from hemocytes of the bacteria-challenged oyster, *Crassostrea gigas*. Gene 303:139–145.

Huang J, Zhang C, Zhuojun M, Liping X, Zhang R. 2007. A novel extra-cellular EF-hand protein involved in the shell formation of pearl oyster. Biochimica et Biophysica Acta 1770:1037–1044.

Humphries JE, Yoshino TP. 2003. Cellular receptors and signal transduction in molluscan hemocytes: connections with the innate immune system of vertebrates. Integr Comp Biol 43:305–312.

Hunter GK, Goldberg HA. 1993. Nucleation of hydroxyapatite by bone sialoprotein. Proc Natl Acad Sci USA 90:8562–8565.

Hunter GK, Goldberg HA. 1994. Modulation of crystal formation by bone phosphoproteins: role of glutamic acid-rich sequences in the nucleation of hydroxyapatite by bone sialoprotein. Biochem J 90:175–179.

Johnstone MB. 2007. A comparative study of molluscan shell proteins with an emphasis on the structure of two phosphoproteins derived from the Eastern oyster, *Crassostrea virginica*. Ph.d. dissertation. Clemson University.

Kawaguchi T, Watabe N. 1993. The organic matrices of the shell of the American oyster *Crassostrea virginica* Gmelin. J Exp Mar Biol Ecol 170:11–28.

Kono M, Hayashi N, Samata T. 2000. Molecular mechanism of the nacreous layer formation in *Pinctada maxima*. Biochem Biophy Res Commun 269:213–218.

Liu H, Liu SF, Ge Y, Liu J, Wang XY, Xie LP, Zhang RQ, Wang Z. 2007. Identification and characterization of a

biomineralization related gene PFMG1 highly expressed in the mantle of *Pinctada fucata*. Biochemistry 46: 844–851.

Mann K, Weiss IM, Andre S, Gabius HJ, Fritz M. 2000. The amino-acid sequence of the abalone (*Haliotis laevigata*) nacre protein perlucin-detection of a functional C-type lectin domain with galactose/mannose specificity. Eur J Biochem 267:5257–5264.

Marin F, Corstjens P, de Gaulejac B, de Vrind-De Jong E, Westbroek P. 2000. Mucins and molluscan calcification – molecular characterization of mucoperlin, a novel mucin-like protein from the nacreous shell layer of the fan mussel *Pinna nobilis* (Bivalvia, pteriomorphia). J Biol Chem 275: 20667–20675.

Miyamoto H, Miyoshi F, Kohno J. 2005. The carbonic anhydrase domain protein nacrein is expressed in the epithelial cells of the mantle and acts as a negative regulator in calcification in the mollusc *Pinctada fucata*. Zool Sci 22: 311–315.

Mount AS. 1999. Nucleation of calcite in the Eastern oyster, *Crassostrea virginica*: biochemical and functional studies of the organic matrix from foliated shell. Ph.D. dissertation. Clemson University.

Mount AS, Wheeler AP, Paradkar RP, Snider D. 2004. Hemocyte-mediated shell mineralization in the Eastern oyster. Science 304:297–300.

Mouries LP, Almeida MJ, Milet C, Berland S, Lopez E. 2002. Bioactivity of nacre water-soluble organic matrix from the bivalve mollusk *Pinctada maxima* in three mammalian cell types: fibroblasts, bone marrow stromal cells and osteoblasts. Comp Biochem Physiol 132B:217–229.

Myers JM, Veis A, Sabsay B, Wheeler AP. 1996. A method for enhancing the sensitivity and stability of Stains-All for phosphoproteins separated in sodium dodecyl sulfate-polyacrylamide gels. Anal Biochem 240:300–302.

Myers JM, Johnstone MB, Mount AS, Silverman H, Wheeler AP. 2007. TEM immunocytochemistry of a 48 kDa MW organic matrix phosphoprotein produced in the mantle epithelial cells of the Eastern oyster (*Crassostrea virginica*). Tissue and Cell 39:247–256.

O'Regan A, Berman J. 2000. Osteopontin: a key cytokine in cell-mediated and granulomatous inflammation. Int J Exp Pathol 81:373–390.

Patel SV. 2004. A novel function of invertebrate collagen in the biomineralization process during the shell repair of Eastern oyster, *Crassostrea virginica*. M.S. thesis. Clemson University.

Rusenko KW, Donachy JE, Wheeler AP. 1991. Purification and characterization of a shell matrix phosphoprotein from the American oyster. In: Sikes CS, Wheeler AP, editors. Surface reactive peptides and polymers. Washington, DC: ACS Books. p 107–124.

Sodek J, Ganss B, McKee MD. 2000. Osteopontin. Crit Rev Oral Biol Med 11:279–303.

Steitz SA, Speer MY, McKee MD, Liaw L, Almeida M, Yang H, Giachelli CM. 2002. Osteopontin inhibits mineral deposition and promotes regression of ectopic calcification. Am J Pathol 161:2035–2046.

Sud D, Doumenc D, Lopez E, Milet C. 2001. Role of water-soluble matrix fraction, extracted from the nacre of *Pinctada maxima*, in the regulation of cell activity in abalone mantle cell culture (*Haliotis tuberculata*). Tissue Cell 33:154–160.

Sudo S, Fujikawa T, Nagakura T, Ohkubo T, Sakaguchi K, Tanaka M, Nakashima K, Takahashi T. 1997. Structure of mollusc shell framework proteins. Nature 387:563–564.

Suzuki M, Murayama E, Inoue H, Ozaki N, Tohse H, Kogure T, Nagasawa H. 2004. Characterization of Prismalin-14, a novel matrix protein from the prismatic layer of the Japanese pearl oyster *Pinctada fucata*. Biochem J 382(Pt 1):205–213.

Takeuchi T, Endo K. 2006. Biphasic and dually coordinated expression of the genes encoding major shell matrix proteins in the pearl oyster *Pinctada fucata*. Mar Biotechnol 8:52–61.

Thompson JB, Paloczi GT, Kindt JH, Michenfelder M, Smith BL, Stucky G, Morse DE, Hansma PK. 2000. Direct observation of the transition from calcite to aragonite growth as induced by abalone shell proteins. Biophys J 79:3307–3312.

Tirapé A, Bacquea C, Brizard R, Vandenbulckec F, Boulo V. 2007. Expression of immune-related genes in the oyster *Crassostrea gigas* during ontogenesis. Dev Comp Immunol 31:859–873.

Wada T, McKee MD, Steitz S, Giachelli CM. 1999. Calcification of vascular smooth muscle cell cultures: inhibition by osteopontin. Circ Res 84:166–178.

Watabe N. 1965. Studies on shell information—Crystal-matrix relationships in the inner layers of mollusk shells. J Ultrastruct Res 12:351–370.

Weiss IM, Kaufmann S, Mann K, Fritz M. 2000. Purification and characterization of perlucin and perlustrin, two new proteins from the shell of the mollusc *Haliotis laevigata*. Biochem Biophys Res Commun 267:17–21.

Wheeler AP, George JW, Evans CA. 1981. Control of calcium carbonate nucleation and crystal growth by soluble matrix of oyster shell. Science 212:1397–1398.

Wheeler AP, Rusenko KW, George JW, Sikes CS. 1987. Evaluation of calcium binding by molluscan shell organic matrix and its relevance to biomineralization. Comp Biochem Physiol 87B:953–960.

Wheeler AP, Rusenko KW, Swift DM, Sikes CS. 1988. Regulation of in vitro and in vivo $CaCO_3$ crystallization by fraction of oyster shell organic matrix. Marine Biol 98:71–80.

Wheeler AP, Low KC, Sikes CS. 1991. $CaCO_3$ crystal-binding properties of peptides and their influence on crystal growth. In: Sikes CS, Wheeler AP, editors. Surface reactive peptides and polymers: discovery and commercialization. Washington, DC: ACS. p 72–84.

Yano M, Nagai K, Morimoto K, Miyamoto H. 2006. Shematrin: a family of glycine-rich structural proteins in the shell of the pearl oyster *Pinctada fucata*. Comp Biochem Physiol 144(Part B):254–262.

Zhang C, Zhang R. 2006. Matrix proteins in the outer shell of mollusks. Mar Biotechnol 8:572–586.

Zhang C, Li S, Ma Z, Xie L, Zhang R. 2006. A novel matrix protein p10 from the nacre of pearl oyster (*Pinctada fucata*) and its effects on both CaCO(3) crystal formation and mineralogenic cells. Mar Biotechnol 8:624–633.

Zhu B, Suzuki K, Goldberg HA, Rittling SR, Denhardt DT, McCulloch CA, Sodek J. 2004. Osteopontin modulates CD44-dependent chemotaxis of peritoneal macrophages through G-protein-coupled receptors: evidence of a role for an intracellular form of osteopontin. J Cell Physiol 198:155–167.